

Tumor microenvironment remodeling by an engineered oncolytic adenovirus results in improved outcome from PD-L1 inhibition

Victor Cervera-Carrascon^{a,b}, Dafne C.A. Quixabeira^a, Joao Manuel Santos^{a,b}, Riikka Havunen^{a,b}, Sadia Zafar^a, Otto Hemminki^{a,c}, Camilla Heiniö^a, Eleonora Munaro^a, Mikko Siurala^{a,b}, Suvi Sorsa^{a,b}, Tuomas Mirtti^{d,e,f}, Petrus Järvinen^g, Markus Mildh^c, Harry Nisen^c, Antti Rannikko^h, Marjukka Anttila^g, Anna Kanerva^{a,h}, and Akseli Hemminki^{a,b,i}

^aCancer Gene Therapy Group, Translational Immunology Research Program and Department of Oncology, University of Helsinki, Helsinki, Finland; ^bTILT Biotherapeutics Ltd, Helsinki, Finland; ^cDepartment of Urology, Helsinki University Hospital, Helsinki, Finland; ^dInstitute for Molecular Medicine Finland (FIMM), University of Helsinki, Helsinki, Finland; ^eDepartment of Pathology, Medicum, University of Helsinki, Helsinki, Finland; ^fDepartment of Pathology, HUSLAB, Helsinki University Hospital, Helsinki, Finland; ^gPathology Unit, Finnish Food Safety Authority (EVIRA), Helsinki, Finland; ^hDepartment of Obstetrics and Gynecology, Helsinki University Central Hospital, Helsinki, Finland; ⁱHelsinki University Hospital Comprehensive Cancer Center, Helsinki, Finland

ABSTRACT

Checkpoint inhibitors have revolutionized cancer therapy and validated immunotherapy as an approach. Unfortunately, responses are seen in a minority of patients. Our objective is to use engineered adenoviruses designed to increase lymphocyte trafficking and cytokine production at the tumor, to assess if they increase the response rate to checkpoint inhibition, as these features have been regarded as predictive for the responses. When Ad5/3-E2F-d24-hTNFα-IRES-hIL2 (an oncolytic adenovirus coding for TNFα and IL-2, also known as TILT-123) and checkpoint inhibitors were used together in fresh urological tumor histocultures, a significant shift toward immune activity (not only tumor necrosis alpha and interleukin-2 but also interferon gamma and granzyme B) and increased T-cell trafficking signals (CXCL10) was observed. *In vivo*, our viruses enabled an anti-PD-L1 (a checkpoint inhibitor) delivering complete responses in all the treated animals (hazard ratios versus anti-PD-L1 alone 0.057 [0.007; 0.451] or virotherapy alone 0.067 [0.011; 0.415]). To conclude, when an engineered oncolytic adenovirus was utilized to modify the tumor microenvironment towards what meta-analyses have pointed as predictive markers for checkpoint inhibitory therapy, the response to them increased synergistically. Of note, key findings were confirmed in fresh patient-derived tumor explants.

KEYWORDS

Oncolytic virus; adenovirus; checkpoint inhibitors; immunotherapy; tumor microenvironment

Introduction

The impressive complete responses seen in some patients receiving immune checkpoint inhibitors (ICIs), and the increasing number of approved indications, are an objective sign of their success in terms of cancer therapy. Even though this is an ongoing golden era for ICIs, the majority of solid tumor patients still do not experience a long-term response. Some patients benefit only for a limited time while the majority derive no detectable benefit, especially when it comes to common types of non-melanoma solid tumors. Thus, ICIs have definitely been validated as an approach, but since a minority of patients benefit from them, there is an unmet clinical need.

An example of such unmet need can be seen in renal cell carcinoma (RCC) for which an anti-PD-1, nivolumab, has been approved for second-line treatment. In a randomized phase 3 trial, the confirmed response rate was 21.5% in the ICI arm versus 3.9% in the everolimus (an inhibitor of the mammalian target of rapamycin) arm. Median overall survival (OS) was 25.0 and 19.1 months, respectively.¹ Another clinical trial combined the use of an ICI (atezolizumab, anti-PD-L1) with an anti-VEGF (sunitinib) drug, increasing the overall response

rate (ORR) to 32% (25% for anti-PD-L1 as monotherapy and 29% for sunitinib as monotherapy).² RCC is a tumor type previously described as “immunogenic” and some patients respond to high dose IL-2 treatment,³ but the majority show no response to immunotherapies. Clear room for improvement exists in most tumor types, since ORR is still low (melanoma 40%,⁴ urothelial carcinoma 21.1%,⁵ non-small-cell lung cancer 19.4%,⁶ hepatocellular carcinoma 14.3%,⁷ among others).

Increasing the frequency of responses to ICIs is now a paramount aim for the entire cancer immunotherapy field. To understand the differences between patients and to correlate those with their clinical outcomes, many retrospective analyses have been performed. The most consistent findings correlate outcome with the presence of tumor-infiltrating lymphocytes (TILs), PD-L1 expression, total mutational burden, and the expression of immunostimulatory cytokines including interferon gamma (IFNγ), tumor necrosis factor alpha (TNFα), and interleukin-2 (IL-2) among others.^{8–14}

T-cell trafficking, PD-L1 expression, and cytokine signatures are features that can be addressed by the use of viral platforms. The era of using oncolytic viruses (OVs) solely for their direct tumor oncolytic ability while ignoring the effect

they have on the immune system has morphed into oncolytic immunotherapy,¹⁵ since human data indicated that the most relevant result of viral oncolysis appears to be related to the induction of anti-tumor immunity.¹⁶ New generation oncolytic viruses are designed taking into account their lytic activity, but more importantly, highlighting their immune-related features such as immunogenic cell death, the release of tumor-associated antigens, pathogen-associated molecular patterns (PAMPs), damage-associated molecular patterns (DAMPs) and upregulation of MHC. Thus, OV_s can stimulate both innate and adaptive immune systems.¹⁷

Besides the intrinsic ability of viruses to interact with the immune system, they can be engineered to express cytokines, enzymes, or other proteins to target certain immune pathways. In short, many current OV_s aim to destroy the tumor by engaging the immune system to do it. Oncolytic replication is also important, but perhaps chiefly because of its immunostimulatory consequences. Ad5/3-E2F-d24-hTNF α -IRES-hIL2 (TILT-123) is an engineered oncolytic adenovirus with chimeric serotype 5/3 designed specifically to be coupled with T-cell-related therapies such as adoptive-cell transfer¹⁸ (such as chimeric antigen receptor [CAR] T-cell therapy¹⁹) or ICIs.²⁰ To go beyond the inherent immunostimulatory activity of the presence of adenovirus in tumors, TILT-123 was tailored to enhance the antitumor effect of CD8 T cells. After infection with the virus, the tumor cell will express virally delivered TNF α and IL-2 genes before dying. These two cytokines are released into the tumor microenvironment to attract T cells toward the tumor to sustain their proliferation and activity.^{21–23} The addition of ICIs would keep newly recruited or locally generated TILs protected from the inhibitory signals exploited by the tumor.

Our main hypothesis is that the use of a genetically modified adenovirus armed with TNF α and IL-2 changes the tumor circumstances toward those seen in patients with the best responses to ICI (“hot tumors,” understood as tumors highly infiltrated with antitumor immune cells), and those changes might help to increase the response rate to checkpoint blockade. To test the abovementioned hypothesis, we used human tumor histocultures and an *in vivo* model allowing us to approach the questions from different angles. These allowed us to study tumor microenvironment remodeling at the cellular and cytokine level but also anti-tumor efficacy and OS.

Materials and methods

Human tumor histocultures from urological tumor samples

Urological samples were collected from surgically removed kidneys and turned into single-cell suspension following the previously described methodology.²⁴ In short, tissues were cut into fragments of an approximate diameter of 5 mm and then incubated overnight in a medium containing various enzymes to create a single-cell suspension that was subsequently plated into 6-well plates. Single-cell cultures were treated with viruses (Ad5/3-E2 F-d24-hTNF α -IRES-hIL2, multiplicity of infection 100), 20 μ g/mL of anti-human PD-L1 (Atezolizumab, Roche,

Basel, Switzerland), or the both in triplicates. Cytokine production and cell viability were assessed after 1, 3, and 7 d.

Histopathology analyses

Hematoxylin and eosin (H&E), and CD8 (clone 4B11, CD8-4B11-L-CE-H, Leica Biosystems, Wetzlar, Germany) stainings were performed on patient samples and analyzed by a trained pathologist. For PD-L1 expression assessment, the PD-L1 VENTANA (SP142) assay (Roche, Basel, Switzerland) was performed by a trained pathologist and scored under routine protocols in the clinical set-up. Histopathological analyses from murine samples were carried out by a veterinary pathologist as described previously.²⁵

Cell viability assay

Human tumor histocultures were treated (as described before) up to 7 d. Cell viability was assessed with “Cell Titer 96 Aqueous One Solution Cell Proliferation Assay” (G3582, Promega, Madison, Wisconsin, USA), following manufacturer indications. The viability of mock-treated cells was set to 100%.

In vivo experiments

To study treatment-induced changes in tumors, 2.5×10^5 B16.OVA melanoma cells were implanted subcutaneously on 4–6 week old female C57BL/6JOLA^{Hsd} mice (Envigo Labs, Huntingdon, UK). Eleven days after engraftment, animals were randomized into groups ($n = 12$ – 14 /group). Then, they received systemic treatments of 0.1 mg of anti-PD-L1 (clone 10 F.9G2, BE0101, BioXCell, Lebanon, New Hampshire, USA) and intratumoral injections of 1×10^8 vp (including equal amounts of Ad5-CMV-mIL2 and Ad5-CMV-mTNF α viruses, non-replicative in mice) on days 0, 1, 3, and 6. PBS was injected intratumorally for groups that did not receive virus. On day 7, 6 animals per group were sacrificed and tumors collected to investigate immune-cell phenotyping and cytokine signatures. The rest of the animals ($n = 6$ – 8 /group) continued to a 90-d OS study, where the treatments continued once every 3 d, until maximum tumor size reached (18 mm) or complete tumor regression.

Cell lines and viruses

B16.OVA, a mouse melanoma cell line was cultured under recommended conditions.²⁰ The cytokine-armed murine adenoviruses’ (Ad5-CMV-mIL2 and Ad5-CMV-mTNF α) construction and production have been described previously²³ and were used in the *in vivo* experiments. For the human tumor histoculture experiments, the oncolytic Ad5/3-E2 F-d24-hTNF α -IRES-hIL2 (known as TILT-123)²¹ was used.

Cytokine analyses

Cell culture medium supernatants coming from tumor histocultures were collected after 1, 3, and 7 d. Sample size for the cytokine analyses was restricted on availability of tumor sample

(mock; $n = 4$, aPD-L1; $n = 6$, virus; $n = 3$, virus+aPD-L1 (S); $n = 2$, virus+aPD-L1 (PB); $n = 0$). The cytokine levels (IFN γ , TNF α , IL-2, IFN β , granzyme B, CXCL10, IL-6, arginase, and TGF- β 1) on the samples were assessed with a custom Legendplex panel (Biolegend, Dedham, Massachusetts, USA) and a Free Active/Total TGF- β 1 detection kit (740488, 740486, and 740487, Biolegend, Dedham, Massachusetts, USA). Cytometric Bead Array Mouse Th1/Th2/Th17 Cytokine kit (560485, BD, Franklin Lakes, New Jersey, USA) was used to study murine tumor samples as described before.²⁰ Both cytokine bead arrays were analyzed with Accuri® (BD, Franklin Lakes, New Jersey, USA). The obtained cytokine values were normalized to total protein concentration of the sample.

PD-L1/2 expression assays

When studying PD-L1 expression dynamics, B16.OVA cells were treated with 1000 U/mL of murine IFN γ (315-05, Peprotech, Stockholm, Sweden), a known inducer for PD-L1 expression. Mock control cells were left untreated. After 24 h of culture, a fraction of the cells were checked for PD-L1 expression and the rest were washed twice with PBS and passed to duplicate 12-well plates. Part of the cells previously treated with IFN γ stopped receiving the treatment (“withdrawn” group) and the other part continued with the treatment (“IFN γ kept” group). The plates were analyzed 24 h and 72 h after the plating.

Similarly, the effect of IFN γ (1000 U/mL), TNF α (1000 U/mL and 10000 U/mL), IL-2 (1000 U/mL and 10000 U/mL), Ad5-luc (1 and 100 vp/cell), Ad5-CMV-mIL2 (1 and 100 vp/cell), Ad5-CMV-mTNF α (1 and 100 vp/cell), or different combinations of those on PD-L1 and PD-L2 expression on B16.OVA cells. These expression levels were studied at 24- and 72-h time points.

Flow cytometry

Cell cultures and tumor samples were processed and labeled as described elsewhere.²⁰ Anti-CD4-FITC (clone GK1.5, 100406, Biolegend, Dedham, Massachusetts, USA), anti-CD3e-PE (clone 145-2C11, 12-0031-82, eBioscience, San Diego, California, USA), anti-CD69-PE-Dazzle (clone HI.2 F3, 104536, Biolegend, Dedham, Massachusetts, USA), anti-CD8-PE-Cy5 (clone 53.6-7, 100710, Biolegend, Dedham, Massachusetts, USA), anti-PD-1-PE-Cy-7 (clone 29 F.1A12, 135216, Biolegend, Dedham, Massachusetts, USA), anti-CD45-FITC (clone 30-F11, 103107, Biolegend, Dedham, Massachusetts, USA), anti-PD-L2-PE (clone MIH5, 558091, BD, Franklin Lakes, New Jersey, USA), anti-Gr-1-PE-Dazzle (RB6-8C5, 108452, Biolegend, Dedham, Massachusetts, USA), anti-CD11b-PE-Cy5 (MI1/70, 101210, Biolegend, Dedham, Massachusetts, USA), anti-PD-L1-PE-Cy7 (TY-25, 107214, Biolegend, Dedham, Massachusetts, USA) were used for flow cytometric analyses under manufacturer’s indications. The analyses were performed with SH800Z cytometer (SONY, Minato, Japan).

Statistical analyses

Tumor growth evolution was studied by a mixed-model analysis of log-transformed tumor volumes with SPSS Statistics 25 (IBM, Armonk, New York, USA). GraphPad (San Diego,

California, USA) software was used to present the data, to analyze OS (Kaplan–Meier, Log-rank Mantel–Cox test), Hazard Ratios (HRs), and 95% confidence intervals (CIs). In addition, GraphPad was used to evaluate the differences between groups in cytometry or cytokine analyses (unpaired t-test with Welch’s correction), correlation analyses between variables (Pearson’s r), over-time evolution of variables (two-way ANOVA), and linear regression. Synergy was calculated using the fractional tumor volume (FTV) method. P values < .05 were considered statistically significant. Data is available upon reasonable request.

Ethics approval and consent to participate

Central Hospital Operative Ethics Committee approved the studies (HUS/850/2017) performed on patients’ material and written informed consent was given by the patients. Experimental protocols for animal studies were reviewed and approved by the ethical committee from the National Animal Experiment Board of the Regional State Administrative Agency of Southern Finland, and all the procedures were carried out in accordance with the recommendations in the Act on the Protection of Animals Used for Scientific or Educational Purpose (497/2013) and Government Decree on the Protection of Animals Used for Scientific or Educational Purposes (564/2013) as well as the European Directive 2010/63/EU.

Results

Oncolytic adenovirus-mediated tumor cell lysis in patient-derived urological tumor histocultures

To understand how oncolytic virotherapy can enable responses to checkpoint inhibitors in solid tumors, three surgically removed tissues were studied. The tumor types (urothelial carcinoma: sample 1. Clear cell renal cell carcinoma: samples 2 and 3) are currently approved²⁶ for anti-PD-L1 treatment or there are Phase III clinical studies showing evidence of benefit for the therapy²⁷. These tumors were pathological grade 3 (sample 2) or 4 (samples 1 and 3) as evaluated from the hematoxylin and eosin staining (Figure 1a). Because one of the primary effects of the virally delivered cargo affects CD8 + T cells, their presence was also assessed (Figure 1b), showing two samples with an immune-excluded (“cold”) phenotype (Samples 1 and 2) and one with an immune-inflamed (“hot”) phenotype (sample 3). In addition, of relevance for anti-PD-L1 targeting, an assay to determine PD-L1 positivity was performed. This showed PD-L1 expression below 5% in immune cells in all samples, making them negative according to the test guidelines (Figure 1c).

After sample processing, a viability assay was performed to measure how the treatments affected the survival of tumor histocultures (Figure 1d). By day 7, a statistically significant decrease in tumor viability was achieved with virotherapy in all three samples when compared with mock or anti-PD-L1 monotherapy ($p < .01$). At that time, the viability of the virally treated groups dropped 62% (95%CI = [54.19; 69.89]) compared with mock and 56% (95%CI = [38.49; 73.39]) when

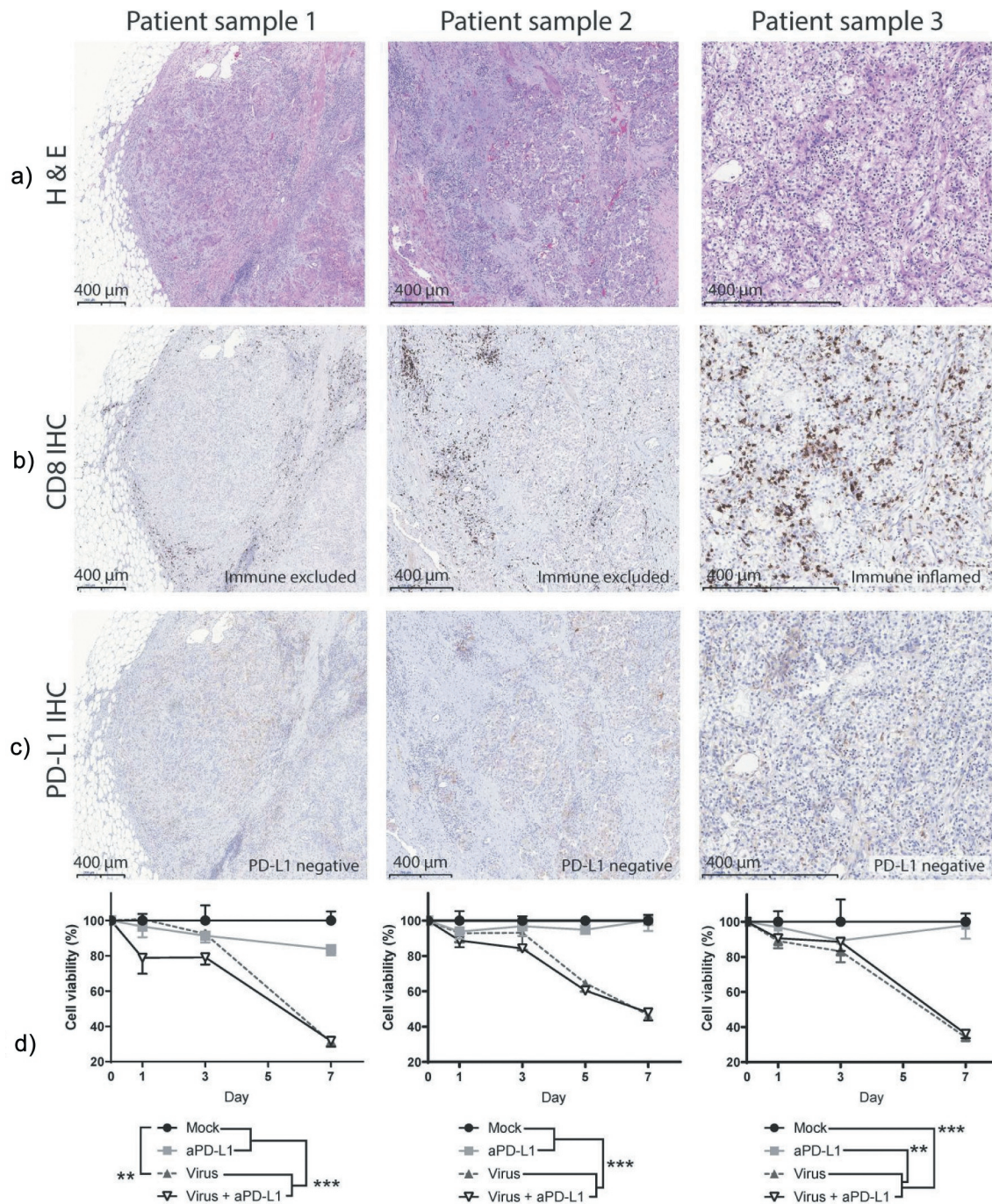


Figure 1. Urological cancer patient-derived samples respond to oncolytic virotherapy despite phenotypical differences. Patient sample 1 is urothelial carcinoma, patient samples 2 and 3 are Clear cell renal cell carcinoma. (a) Hematoxylin and Eosin staining performed on the paraffin-embedded samples. (b) CD8 immunohistochemistry. (c) PD-L1 immunohistochemistry. (d) MTS viability assay after *ex vivo* treatment of the histocultures. Statistical significances are shown for day 7 calculated by unpaired t-test with Welch's correction (** $p < .01$; *** $p < .001$). Mean and standard error of the mean (SEM) are shown.

compared with anti-PD-L1-treated samples. Already on day 1, there were significant reductions on cell viability in two of the samples, when virus and anti-PD-L1 were given together.

Oncolytic virotherapy triggers a broad immunostimulatory response in human urological tumor histocultures

We also studied the histocultures for the impact of the treatments on cytokine levels (Figure 2). Because of the heterogeneity

typically seen in actual patient tumors, cytokine levels between samples varied. Nevertheless, groups receiving virotherapy displayed a clear trend for increased expression of immunostimulatory cytokines (IFN γ , TNF α , IL-2, granzyme B, and CXCL10) (Figure 2a-f, Supp. Figure 2). Regarding IFN γ , increased production was achieved when Ad5/3-E2 F-d24-hTNF α -IRES-hIL2 was administered together with anti-PD-L1 in comparison with "Mock" ($p = .0182$) and "anti-PD-L1" alone groups ($p = .0181$). The "Virus" alone group had a similar trend ($p = .068$). TNF α and IL-2 production were also increased in

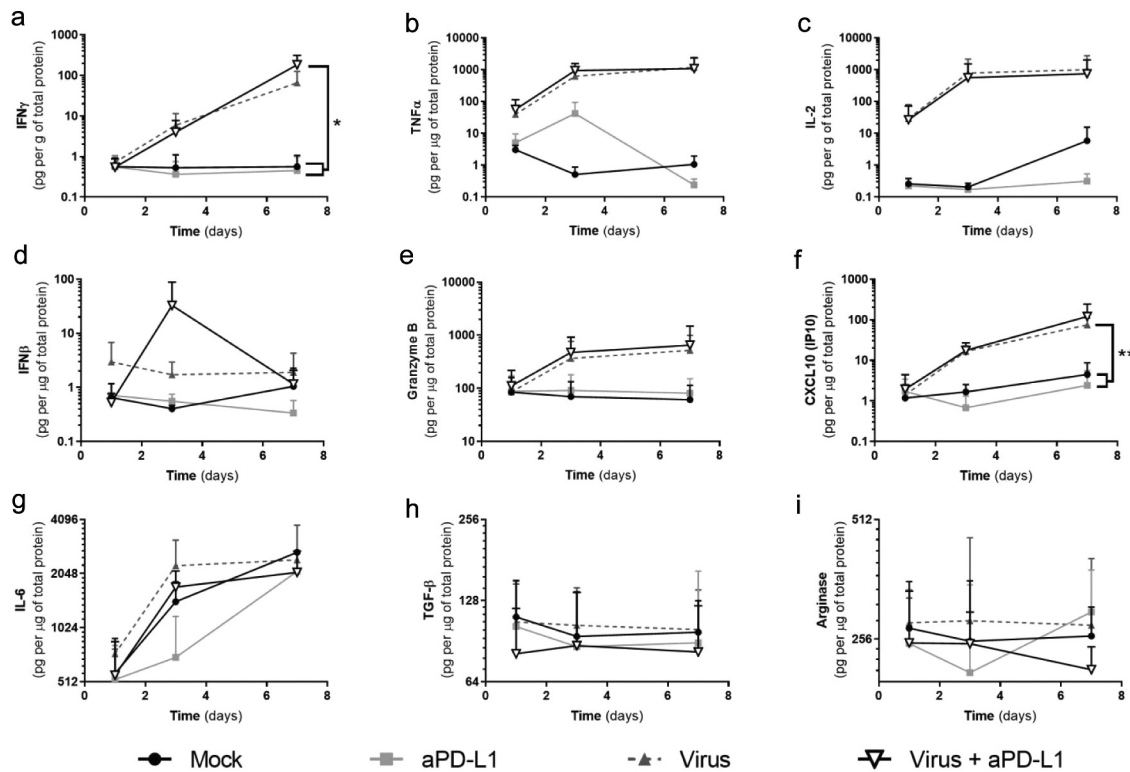


Figure 2. Responses to virotherapy and checkpoint inhibitor treatments at the cytokine level across 7 d of treatment. Expression values from three individual patient-derived tumor histocultures were plotted together. (a) IFN γ . (b) TNF α . (c) IL-2. (d) IFN β . (e) Granzyme B. (f) CXCL10. (g) IL-6. (h) TGF β . (i) Arginase. Statistical significances calculated by two-way ANOVA. (* $p < .05$; ** $p < .01$). Mean and standard error of the mean (SEM) are shown.

virally treated groups and the differences were significant when samples were analyzed individually (Supp. Figure 2b-c). IFN β production, on the other hand, was not as clearly affected as the other immunostimulatory cytokines, except for a peak in production on day 3 with the double treatment.

Granzyme B and CXCL10 had higher expression values in virally treated groups. The expression of these two proteins correlated with IFN γ expression (IFN γ /Granzyme B: $r = 0.629$ [0.376; 0.792], $p < .001$. IFN γ /CXCL10: $r = 0.494$ [0.198; 0.708], $p = .002$). CXCL10 expression was significantly increased in “Virus” group when compared with “Mock” ($p = .003$) and with “anti-PD-L1” ($p = .002$). Treatment with aPD-L1 alone did not affect the expression of immunostimulatory markers compared with “Mock” group.

Statistically significant reduction of IL-6 was achieved by “anti-PD-L1” group and “Virus + anti-PD-L1” when compared with “Mock” or “Virus” in two out of three samples (Supp. Figure 2g). Regarding immunosuppressive mediators (TGF- β , and arginase), effects of treatments are not as clear as for the stimulatory ones. For TGF- β (Supp. Figure 2h) significant decreases were achieved in all samples for the “Virus + anti-PD-L1” group, while for “anti-PD-L1” group this was seen only in one sample. Arginase was included in the panel, despite the fact not being a cytokine but an enzyme affecting immune activity. For this enzyme, one sample displayed reduced expression in the “anti-PD-L1” group and “Virus + anti-PD-L1” when compared with “Mock” or “Virus” (Supp. Figure 2i).

Treatment-induced immunostimulatory cytokine production relates to the reduction of viability in solid tumor samples

To compare the differential expression of markers in tumor histocultures on day 7, average fold change compared with “Mock” was plotted side-by-side (Figure 3a,b). Among the six stimulatory markers analyzed, the increase in TNF α and IL-2 expression is likely related, at least partially, to viral expression of the transgenes and cannot be distinguished from the endogenous production. Of note, there was more than a 1000-fold increase in TNF α expression and around a 100-fold increase for IL-2. Regarding IFN γ , virally treated groups displayed over a 100-fold increase compared with mock conditions. Interestingly, the addition of anti-PD-L1 to virus treatment results in 10 times higher expression when compared to virus alone (1000 times higher than in “Mock”). Additionally, virus treatments induced an average of 25-fold increase in CXCL10 levels.

The treatments had a less drastic effect on the expression levels of TGF- β , and arginase (Figure 3b). Anti-PD-L1 therapy seemed to reduce the amount of TGF- β , while arginase expression was reduced only when both the virus and the checkpoint inhibitor were given together. To compare the presence of the measured immune-suppressors and immune-stimulators present at the tumor, average values of TGF- β and arginase were plotted against average values of IFN γ , IFN β , granzyme B, and CXCL10 (Figure 3c), to have an overall view on the two types of signals for each group. The use of both treatments together

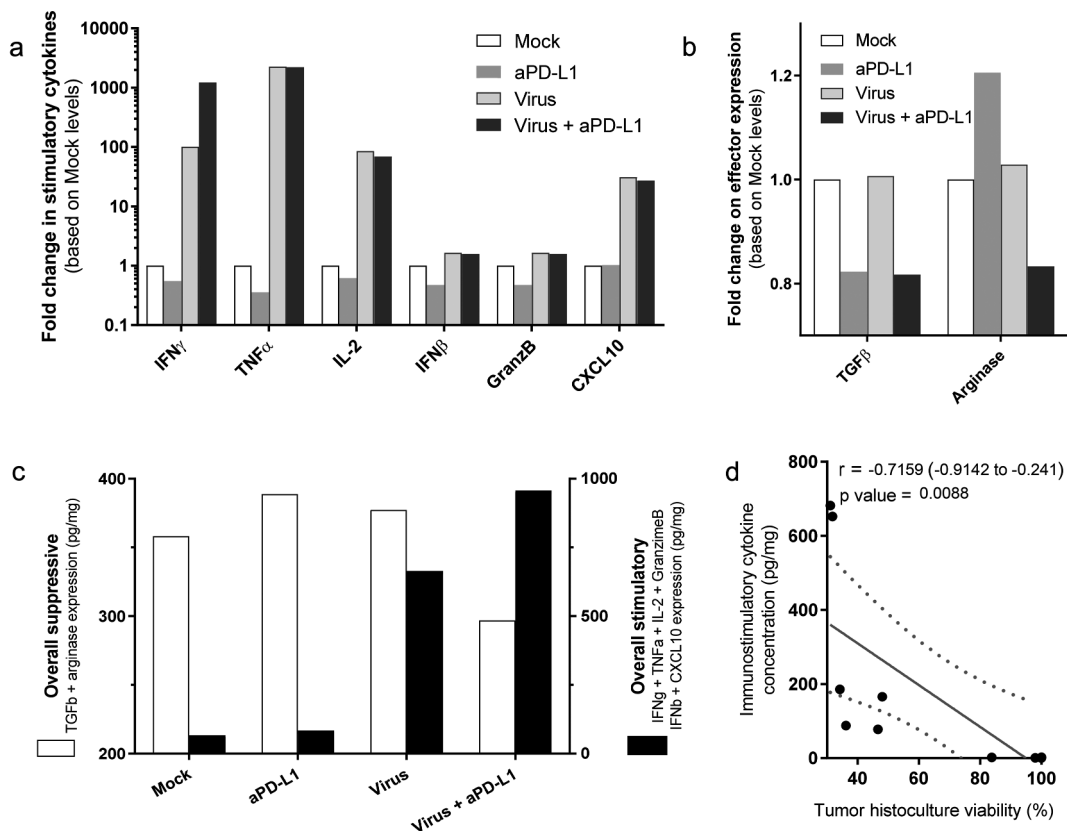


Figure 3. Analyses of grouped cytokine responses to virotherapy and checkpoint inhibitor treatments on day 7. Expression values from three different patient-derived tumor histocultures were plotted together. (a) Fold change in immunostimulatory cytokines. (b) Fold change in immunosuppressive effectors. (c) Overall suppression (including TGF- β and arginase) vs overall stimulation (including IFN γ , IFN β , granzyme B, and CXCL10). (d) Pearson's r correlation between immunostimulatory cytokine expression and tumor histoculture viability.

induced a decrease in immune suppression, delivered by the checkpoint inhibitor, and immunostimulation via virotherapy. An inversely proportional correlation was seen between the production of immunostimulatory cytokines and the tumor histoculture cell viability ($r = -0.716 [-0.914; -0.241]$, $p = .009$) (Figure 3d). No correlation was found between cell viability and immunosuppressive cytokines.

TNF α and IL-2 expressing adenoviruses enable anti-PD-L1 therapy in vivorendering 100% complete response rate

Next, we aimed to assess if immune-stimulation triggered by the virus and reduced suppression achieved by anti-PD-L1 was reproducible *in vivo*. In addition, we wanted to study the impact of tumor immune remodeling in terms of anti-tumor efficacy (Figure 4a). To understand the interaction between the treatments, two groups were treated with viruses and checkpoint inhibitors but with different administration regimens; while one group received both treatments simultaneously (S) the other received the virus treatment, in a “prime and boost” manner (PB). In the prime and boost group, the virus is given without anti-PD-L1 for two rounds and then anti-PD-L1 is included in the treatment.

The two groups that received viruses and anti-PD-L1 together displayed better results in terms of survival than the other groups (Figure 4b). Particularly, when the viruses (intratumoral) were administered simultaneously with anti-PD-L1 (intravenous), 100% complete response rate was achieved. The “Virus + aPD-

L1 (s)” group had significantly longer survival than any other group ($p < .001$ against “Mock,” $p = .007$ against “aPD-L1,” $p = .005$ against “Virus” and $p = .025$ against “Virus + aPD-L1 (PB)”). The hazard ratio of the “Virus + aPD-L1 (s)” strategy was superior over any other group studied (HR = 0.033 [0.006; 0.181] against “Mock,” HR = 0.057 [0.007; 0.451] against “aPD-L1,” HR = 0.067 [0.011; 0.415] against “Virus” and HR = 0.104 [0.014; 0.752] against “Virus + aPD-L1 (PB)”).

The “prime and boost” approach resulted in significantly longer OS ($p < .001$) and lower HR (0.059 [0.012; 0.290]) over mock. Virotherapy or checkpoint inhibitor monotherapy resulted in circa 33% CR. OS with virotherapy alone was statistically improved over mock ($p = .016$), with a lower HR (0.180 [0.044; 0.727]). Individual tumor volume graphs were also plotted (Figure 4c) and synergistic effects were seen following dual therapy (Supp. Figure 3) as early as day 5. At day 90 after the treatments started, some of the animals that had undergone a complete response had a scar tissue in the peritumoral area. After the sacrifice of the animals, scars were collected and analyzed by a pathologist (Supp. Figure 4), who reported the presence of melanophages, plasma cells, and lymphocytes, but no malignant cells.

Virotherapy increases the amount of active CD8T cells intratumorally in vivo

To assess the early immunological impact of the treatments, six animals per group were randomly selected, sacrificed, and

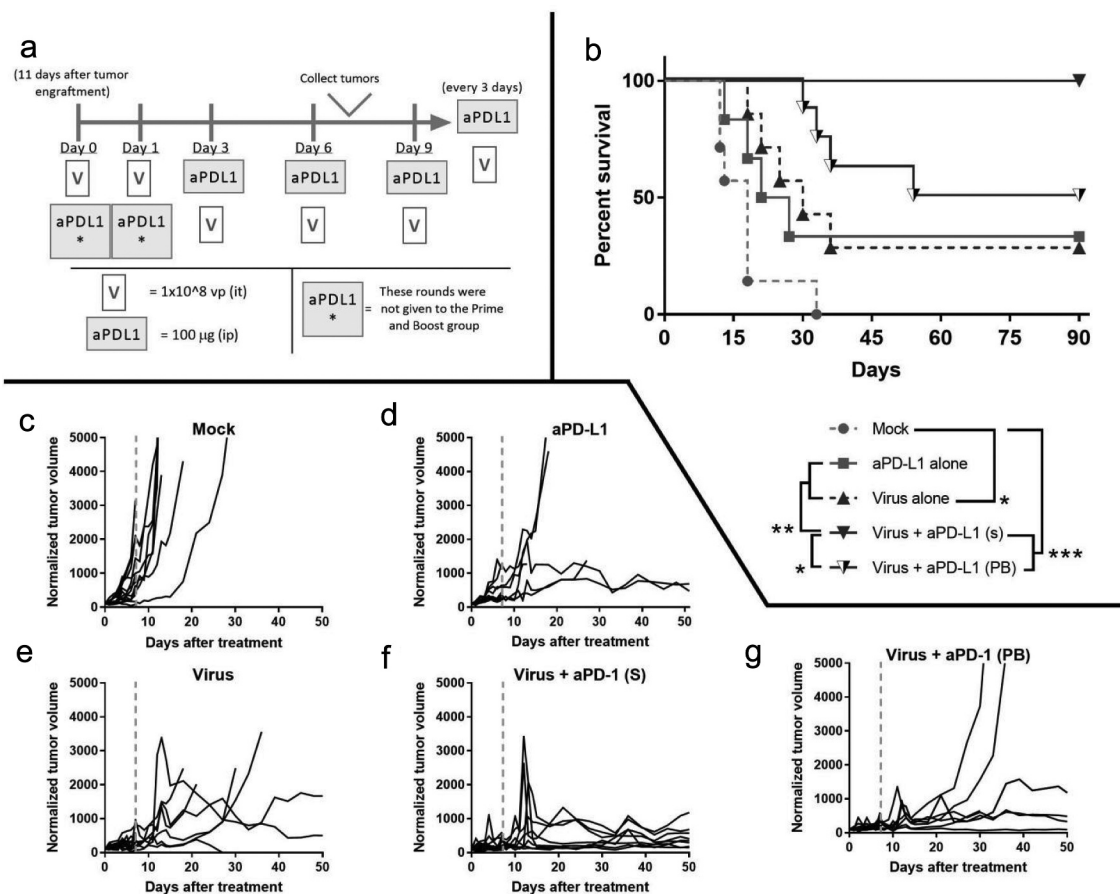


Figure 4. *In vivo* testing of virotherapy to enable checkpoint inhibitory therapy. (a) Experimental design: 66 animals with B16.OVA tumors started treatments on day 0. Thirty of them were sacrificed on day 7 post-treatment (gray-dashed line) and tumors collected while the rest were kept alive for a survival experiment, with more rounds of treatments until tumors regressed completely or death (S: simultaneous administration of virus and aPD-L1, PB: prime and boost). (b) Overall survival (Kaplan-Meier, Log-rank Mantel-Cox test). (c-g) Individual tumor growth lines. (* $p < .05$; ** $p < .01$, *** $p < .001$).

tumors collected on day 7. Virotherapy increased the proportion of CD8 + T cell trafficking to the tumor (Figure 5a). Statistical significances were achieved for the “Virus” group ($p = .011$) and in the “virus + aPD-L1 (PB)” ($p = .003$) when compared with “Mock,” which had almost no infiltration of CD8+ cells. The other virally treated group, “virus + aPD-L1 (s),” also had a sub-significant increase in CD8+ T cells ($p = .093$), but the highest mean levels among all the groups. Regarding the total CD8 T-cell population present in tumors, there were more activated cells (based on CD69 expression) when the animals were treated with virotherapy ($p < .05$ for all the virally treated groups) (Figure 5b).

Upon measuring the proportion of active CD8 T cells out of total cells, the average values in virally treated groups were up to 100 times higher (virus + aPD-L1 (s)) when compared with “Mock” values (Figure 5c). The percentage of PD-1 positive cells among tumor-infiltrating CD8 T cells was nearly 100% for all groups (Figure 5d). When PD-1 expression intensity was addressed, significant differences were observed in the groups receiving viral vectors (Figure 5e). In fact, PD-1 expression intensities correlated with the percentage of active T CD8 cells ($r = 0.927$ [0.849; 0.9655], $p < .0001$) (Supp. Figure 5a).

The CD8/CD4 ratio increased in treated groups (Figure 5f). There is also a trend toward an increase in CD4+ cells in the groups treated with both virus and ICI (Figure 5g), but in a less

steep manner than CD8+ cells. Regarding the overall trafficking of leukocytes (defined here as CD45+ cells), tumors treated with viruses displayed a significant increase (Figure 5h).

In the context of anti-PD-L1 therapy, it is especially relevant to understand the expression of tumor PD-L1 and PD-L2. For that reason, it was studied if any of the cytokines encoded by the viruses, the viruses themselves, or their combination was able to upregulate PD-L1 (Supp. Figure 6a) or PD-L2 (Supp. Figure 6b). Unlike IFN γ , the cytokine-producing virus or the components separately did not upregulate PD-L1 or PD-L2. Interestingly, induction achieved with IFN γ was reversible as the levels returned to the baseline after 72 h of culturing without IFN γ (Supp. Figure 6c-e). In accordance, the groups with a higher presence of active CD8 T cells and higher IFN γ production (see below) displayed a higher percentage of PD-L1+ tumor cells (Figure 5i) and the highest PD-L1 intensity (Figure 5j).

Alteration of PD-L1 expression by IFN γ did not occur in the leukocyte fraction. The only group with a statistically significant increase in the percentage of PD-L1+ cells (Figure 5k) and PD-L1 intensity (Figure 5l) was the one treated with anti-PD-L1 monotherapy.

PD-L2 expression was also studied (Supp. Fig 7a-d). In this case, virus monotherapy induced a significant increase in the percentage of positive cells when compared with every other

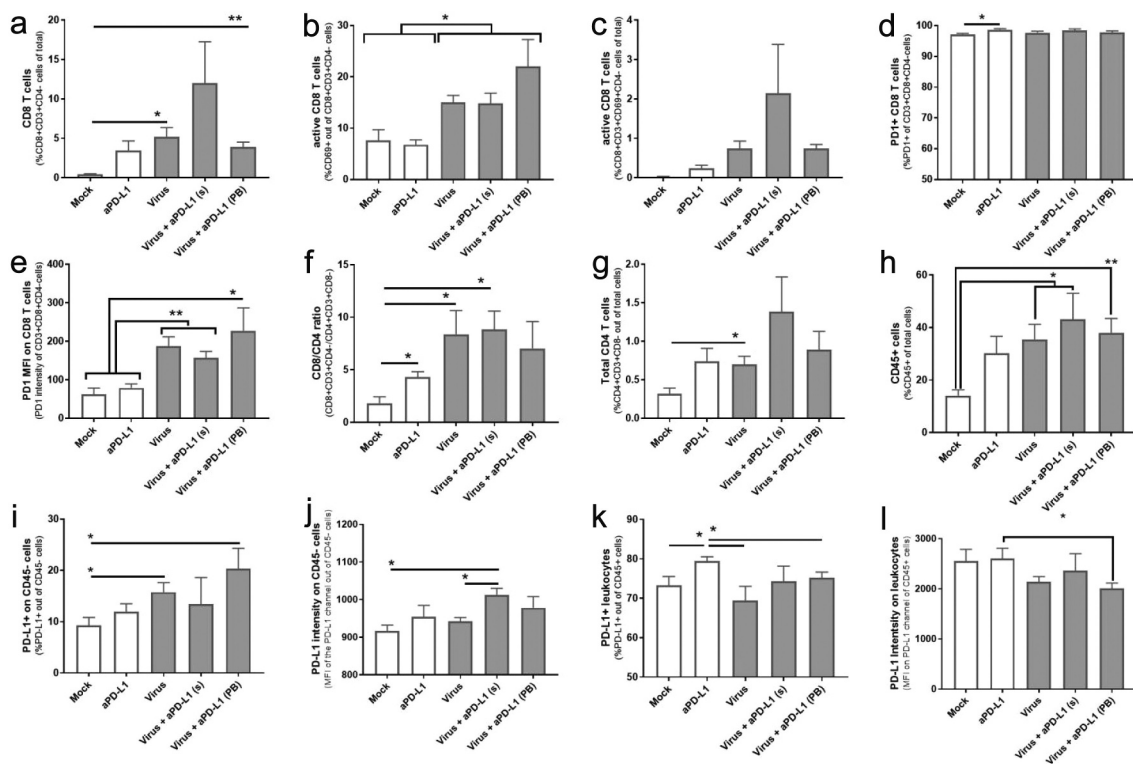


Figure 5. *In vivo* responses to virotherapy and checkpoint inhibitor treatments on day 7 analyzed by flow cytometry. (a) %CD8 + T cells out of total cells. (b) %CD69+ out of CD8 + T cells. (c) %CD69+ CD8 + T cells out of total cells. (d) %PD-1+ out of CD8 T cells. (e) PD-1 intensity on CD8 + T cells. (f) CD8/CD4 ratio. (g) %CD4+ cells out of total cells. (h) %CD45+ cells out of total cells. (i) %PD-1+ cells out of CD45- cells. (j) PD-1 intensity on CD45- cells. (k) %PD-1+ cells out of CD45+ cells. (l) PD-1 intensity on CD45+ cells. Mean and standard error of the mean (SEM) are shown. Differences between groups calculated by (*p < .05; **p < .01, ***p < .001).

group in both CD45- and CD45+ populations (“tumor” and “leukocyte,” respectively). It is noticeable that both monotherapies increased PD-L2 signals, but that increase did not occur when therapies were administered together. PD-L2 effects are of unknown significance at this point, since the role of this molecule in immunotherapy is unclear in general.

Myeloid-derived suppressor-like cells (MDSCs) constitute another relevant cell population due to their ability to disable immune activity. For that reason, they were studied in terms of suppressive ligands (Supp. Fig 7e-j). Their inherent suppressivity was observed as all of them expressed PD-L1 and PD-L2, the levels being more intense in the group treated with virus as monotherapy.

Oncolytic virotherapy triggers a broad immunostimulatory cytokine response *in vivo*

Similarly, as done with urological human tumor histocultures, we proceeded to study the differential expression of immunostimulatory and immune-suppressive cytokines in melanoma tumors collected 7 d after treatments started. A trend for increased IFN γ production was observed for the “virus+aPD-L1 (S)” group, which was less marked for groups treated with monotherapies (Figure 6a). The IFN γ production correlated with the presence of CD8 T cells in the tumors ($r = 0.720$ [0.330; 0.900]) (Suppl Figure 5b).

Regarding TNF and IL-2, virally treated animals expressed high levels (Figure 6b-c), most likely deriving from the viruses at least in part. Suppressive cytokines, such as IL-4 and IL-10,

seemed to be higher in “Mock” conditions, while both checkpoint inhibitors and viruses reduced their expression (Figure 6d-f). When immunosuppressive and immunostimulatory cytokines were plotted together, we did not observe remarkable differences between the two groups receiving virotherapy, but there was a trend toward lower immunosuppression and increased immunostimulation when comparing those groups with “Mock” and “anti-PD-L1” (Figure 6g).

Another correlation was found between the presence of active (CD69+) CD8 T cells and IFN γ in the tumor microenvironment ($r = 0.782$ [0.451; 0.924]) (Figure 6h). The groups with higher IFN γ also displayed increased PD-L1 expression on tumor cells (Figure 5i,j).

Discussion

In this study, we show how a viral platform coding for TNF α and IL-2 has a considerable impact on the immune tumor microenvironment, which led to higher responses in the context of anti-PD-L1 checkpoint inhibition. Similar results were observed both in human urological clinical sample histocultures (renal cell cancer and urothelial cancer) and *in vivo*, resulting in improved tumor growth control and survival. It is noteworthy that both monotherapies had a positive effect. When they were used together, synergistic antitumor control was clear in the context of tumor control when studied in immunocompetent models, and beneficial outcomes were observed when analyzing immune mediators. Importantly, checkpoint inhibition prevented the switching-off of crucial

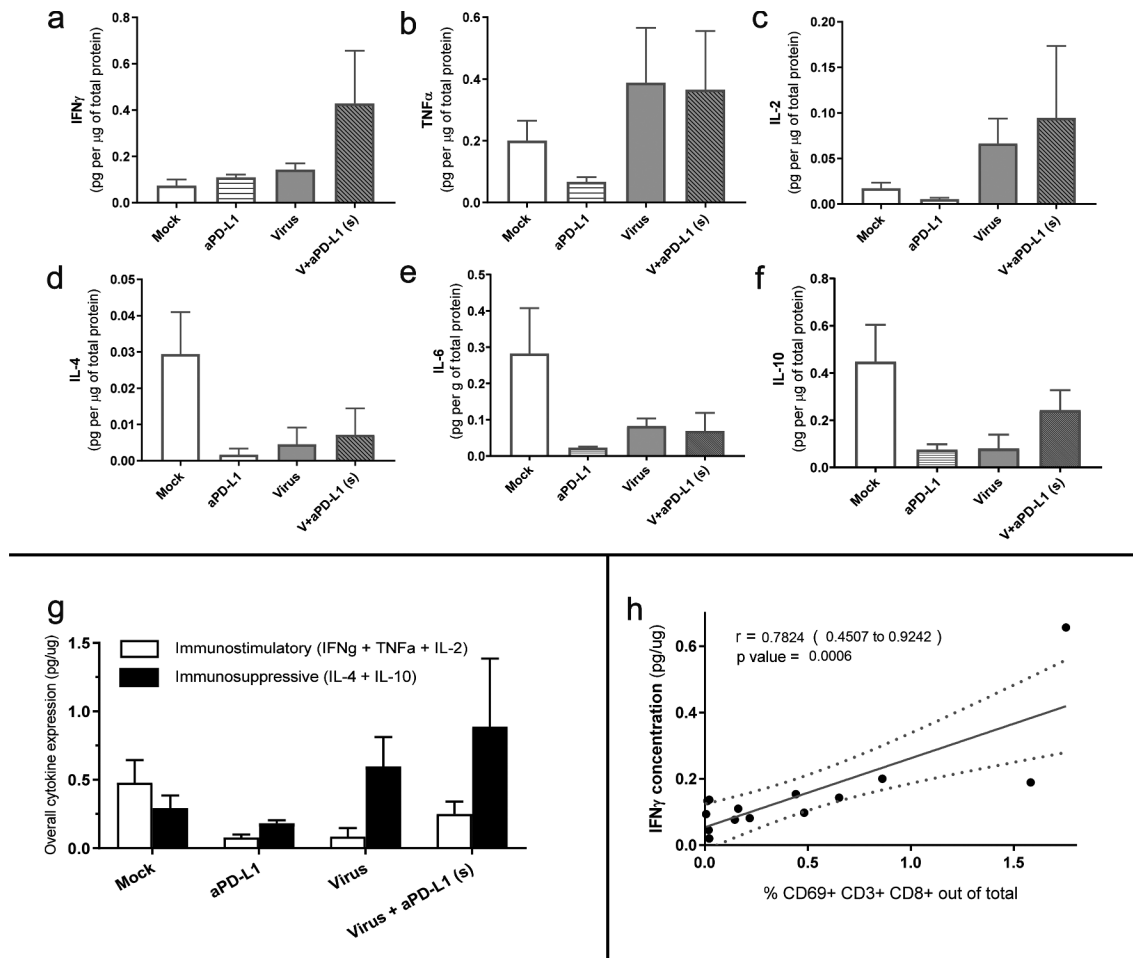


Figure 6. Responses to virotherapy and checkpoint inhibitor treatments at the cytokine level from *in vivo* experiment on day 7. (a) IFN γ production. (b) TNF production. (c) IL-2 production. (d) IL-4 production. (e) IL-6 production. (f) IL-10 production. (g) Overall suppression (including IL-4 and IL-10) vs overall stimulation (including IFN γ , TNF, and IL-2). (h) Correlation analysis between IFN γ production and active T cells.

virus-mediated anti-tumor immune responses. It was only when both aspects were taken into account (activation and prevention of de-activation) that the immune system was able to completely eradicate tumors.

In patients, complete responses are quite rare, partial responses are more common, but even taken together, ORR with ICIs are between 10–40% following monotherapy in most solid tumor types. However, it has been noted that TIL presence^{8,9} and upregulated inflammatory cytokine signature^{11–13} are among the strongest predictive factors. In this regard, it is potentially important that the studied viral platform was able to make “cold” tumors “hot,” to enable effective ICI therapy, for an increased response rate and survival. In animal studies, we observed how the presence of TILs increased after virus treatment, and rose further when combined with a checkpoint inhibitor, showing again the rationale for their combination. This finding is especially relevant in the model used, where the presence of CD8 T cells is near zero in Mock conditions. The effect of the approach in inducing CD8 trafficking to solid tumors was later validated in a different *in vivo* model (Supp. Figure 8). The ability of the TNF α and IL2 coding adenovirus to increase TIL trafficking towards the tumor has been previously described by immunohistochemistry¹⁹ and SPECT/CT.²³ In tumor histocultures, groups receiving virotherapy also showed higher

expression of CXCL10, a chemokine able to promote TIL trafficking.²⁸ With regard to inflammatory cytokine signatures, extensive upregulation was seen both *ex vivo* and *in vivo*.

Other relevant predictive factors are total mutational burden and PD-L1 expression. The mutational burden relates to the probability of immune responses.^{29,30} In this regard, virotherapy probably does not increase or reduce the mutational burden actively, but it has been shown that oncolysis is a mechanism for releasing neoantigens, enhancing their availability to antigen-presenting cells.^{31,32} PD-L1 expression has been used as an indication-defining marker for some tumor types such as non-small-cell lung cancer.³³ However, its baseline expression is not a fully reliable marker.^{10,12,34} The fact that PD-L1 can be expressed both on tumor and immune cells lowers its predictive value. Additionally, PD-L1 expression could imply different things if it is present as a response to IFN γ or because of epigenetic dysregulation indicating immunosuppression.³⁵

In our studies, we observed that PD-L1 was upregulated in tumor cells in those groups with higher expression of IFN γ . This observation raised the question whether PD-L1 upregulation could be explained by direct IFN γ exposure or by some other component of the treatment. To address this issue, we exposed cancer cells to treatment components (backbone

viruses and recombinant TNF α /IL-2, altogether and separately) and IFN γ . We observed that IFN γ stimulus directly produced PD-L1 upregulation on tumor cells but the same did not occur with the rest of the elements involved in the treatments.

In the previous work,²⁰ we addressed the issue of the sequencing administration of virus and anti-PD-1 ICI. We showed that delaying the administration of anti-PD-1 was beneficial for anti-tumor effects, and provided some speculation on the mechanism of the prime-and-boost. In contrast, our results reported here suggest that for PD-L1 blockade simultaneous administration is more effective. Zamarin, D et al.³⁶ arrived at similar conclusions when using Newcastle Disease Virus in combination with anti-PD-L1. A possible mechanistic explanation is that the first wave of PD-L1 upregulation in the tumor is related to a virotherapy-induced innate cytokine-mediated response, while after 4–5 d, when PD-1-positive lymphocytes get to the tumor, the adaptive responses trigger another wave of PD-L1 upregulation. This hypothesis suggests that PD-1 blockade would be needed only after 4–5 d, while PD-L1 blockade is useful from the moment the virus is delivered into the tumor. Another plausible explanation on the difference between antibodies could be that the anti-PD-L1 used here is able to trigger antibody-dependent cellular cytotoxicity while the anti-PD-1 used previously is not as suggested by Dahan, R. et al.³⁷ It is of importance to note that not all ICIs are alike when it comes to combination use with oncolytic viruses. Preclinical studies can be useful in providing a rationale for clinical translation.

Combination immunotherapy is being widely explored and the use of OV with ICIs has produced promising results in early clinical trials.^{38,39} One of the most encouraging approaches features the combination of talimogene laherparepvec (herpes virus expressing granulocyte-monocyte colony-stimulating factor (GM-CSF)) with pembrolizumab (anti-PD-1).⁴⁰ This study reported an increase in response rate (when compared with historical ICI-treated cohorts) without any major increase in toxicity. A phase 3 trial with this approach is ongoing (NCT02263508). It also sets as a promising precedent for the combination of these two immunotherapies.

Unlike talimogene laherparepvec, which targets antigen-presenting cells, the virus used in this work (Ad5/3-E2F-d24-hTNF α -IRES-hIL2 (TILT-123)) was designed in a data-driven manner to enable T cells and T-cell therapies including ICI.^{21,22} TNF α , and IL-2 have a direct effect on effector T cells, while GM-CSF has only indirect effects. This may be a critical advantage in the context of T-cell therapies and ICI. In a complementary setting, we compared the virus coding for TNF α and IL-2 to the unarmed version, showing the critical importance of the transgenes in reshaping the immune microenvironment.²⁴ At the preclinical level, the use of virotherapy together with ICI has been studied by others³⁹ but, achieving 100% OS and 100% tumor control rate in this model is an infrequent achievement. Another relevant feature regarding the experimental design used in the *in vivo* part of this study is that we allowed immunosuppression to develop by allowing tumors to grow longer before initiating therapy, as compared with other studies in the same model.^{36,41}

Nevertheless, our study has some limitations. First, there are no optimal models to test the effect of both treatments. Human

ex vivo tumor histocultures are an acceptable way to study tumor oncolysis and the local impact of the therapies, but the entire immune system is not present. Thus, cell trafficking and generation of adaptive responses are not possible. Regarding animal models, murine cells are not susceptible to adenoviral replication. Thus, even if the transgenes are expressed and the immune activation is achieved, late stages of the viral cycle do not occur, and there is practically no production of new viral particles.⁴² Another model sometimes considered is the Syrian hamster (*Mesocricetus auratus*), as it supports human adenovirus replication and oncolysis.⁴³ Unfortunately, there are no checkpoint inhibitory antibodies available to study the combination with the virus.

In conclusion, we have described how an adenoviral platform coding for TNF α and IL-2 can be used to increase responses to PD-L1. The mechanism relates to the broad upregulation of stimulatory cytokines (IFN γ , IFN β , granzyme B, and CXCL10 besides the virally produced TNF α and IL-2) and the attraction of active CD8 T cells and other leukocytes to the tumor. These changes in the tumor make them resemble immunologically “hot” tumors, which often respond to ICIs. Understanding what makes patients respond and extending this knowledge to other patients will expand the utility of tumor immunotherapy to larger patient populations. The data provided here set the stage for clinical translation of TILT-123 with anti-PD-L1.

Acknowledgments

We thank Susanna Grönberg-Vähä-Koskela, Riikka Kalliokoski, and Minna Oksanen for their assistance during the study. The Biomedicum Flow Cytometry Core Facility and the Tissue Preparation and Histochemistry Unit (University of Helsinki), as well as the Laboratory Animal Centre (University of Helsinki), are appreciated for their technical support. We are grateful for Tiina Gyllenberg, Hanna Kangasmäki, and the staff at the Docrates Cancer Clinic for their kind assistance.

Disclosure of potential conflicts of interest

A.H. is a shareholder in Targovax ASA (Oslo, Norway) and in TILT Biotherapeutics Ltd. (Helsinki, Finland). A.H., M.S., R.H., S.S., J.M.S., and V.C.C. are employees of TILT Biotherapeutics Ltd. Other coauthors declare no potential conflict of interest.

Funding

This study was supported by Marie Skłodowska-Curie Innovative Training Networks (ITN-EID VIRION H2020-MSCA-ITN-2014 project number 643130), Jane and Aatos Erkko Foundation, HUCH Research Funds (EVO), Sigrid Juselius Foundation, Finnish Cancer Organizations, University of Helsinki, Novo Nordisk Foundation, Päivikki and Sakari Sohlberg Foundation, The Finnish Society of Sciences and Letters, and TILT Biotherapeutics Ltd.

ORCID

Victor Cervera-Carrascon  <http://orcid.org/0000-0001-6684-3666>
 Tuomas Mirtti  <http://orcid.org/0000-0003-0455-9891>
 Petrus Järvinen  <http://orcid.org/0000-0002-3751-4609>
 Antti Rannikko  <http://orcid.org/0000-0002-4261-3484>

References

- Xu JX, Maher VE, Zhang L, Tang S, Sridhara R, Ibrahim A, Kim G, Pazdur R. Approval Summary: FDA. Nivolumab in advanced renal cell carcinoma after anti-angiogenic therapy and exploratory predictive biomarker analysis. *Oncologist*. 2017;22:311–317. doi:10.1634/theoncologist.2016-0476.
- McDermott DF, Huseni MA, Atkins MB, Motzer RJ, Rini BI, Escudier B, Fong L, Joseph RW, Pal SK, Reeves JA, et al. Clinical activity and molecular correlates of response to atezolizumab alone or in combination with bevacizumab versus sunitinib in renal cell carcinoma. *Nat Med*. 2018;24:749–757. doi:10.1038/s41591-018-0053-3.
- Itsumi M, Tatsugami K. Immunotherapy for renal cell carcinoma. *Clin Dev Immunol*. 2010;2010:284581. doi:10.1155/2010/284581.
- Lugowska I, Teterycz P, Rutkowski P. Immunotherapy of melanoma. *Contemp Oncol*. 2018;22:61–67.
- Bellmunt J, de Wit R, Vaughn DJ, Fradet Y, Lee J-L, Fong L, Vogelzang NJ, Climent MA, Petrylak DP, Choueiri TK, et al. Pembrolizumab as second-line therapy for advanced urothelial carcinoma. *N Engl J Med*. 2017;376:1015–1026. doi:10.1056/NEJMoa1613683.
- Lim SH, Sun J-M, Lee S-H, Ahn JS, Park K, Ahn M-J. Pembrolizumab for the treatment of non-small cell lung cancer. *Expert Opin Biol Ther*. 2016;16:397–406. doi:10.1517/14712598.2016.1145652.
- El-Khoueiry AB, Sangro B, Yau T, Crocenzi TS, Kudo M, Hsu C, Kim TY, Choo SP, Trojan J, Welling THR, et al. Nivolumab in patients with advanced hepatocellular carcinoma (CheckMate 040): an open-label, non-comparative, phase 1/2 dose escalation and expansion trial. *Lancet*. 2017;389:2492–2502. doi:10.1016/S0140-6736(17)31046-2.
- Tumeh PC, Harview CL, Yearley JH, Shintaku IP, Taylor EJ, Robert L, Chmielowski B, Spasic M, Henry G, Ciobanu V, et al. PD-1 blockade induces responses by inhibiting adaptive immune resistance. *Nature*. 2014;515:568–571. doi:10.1038/nature13954.
- Nishino M, Ramaiya NH, Hatabu H, Hodi FS. Monitoring immune-checkpoint blockade: response evaluation and biomarker development. *Nat Rev Clin Oncol*. 2017;14:655–668. doi:10.1038/nrclinonc.2017.88.
- Chen DS, Mellman I. Elements of cancer immunity and the cancer-immune set point. *Nature*. 2017;541:321–330. doi:10.1038/nature21349.
- Ribas A, Robert C, Hodi FS, Wolchok JD, Joshua AM, Hwu W-J, Weber JS, Zarour HM, Kefford R, Loboda A, et al. Association of response to programmed death receptor 1 (PD-1) blockade with pembrolizumab (MK-3475) with an interferon-inflammatory immune gene signature. *J Clin Oncol*. 2015;33:3001. doi:10.1200/jco.2015.33.15_suppl.3001.
- Herbst RS, Soria JC, Kowanzet M, Fine GD, Hamid O, Gordon MS, Sosman JA, McDermott DF, Powderly JD, Gettinger SN, et al. Predictive correlates of response to the anti-PD-L1 antibody MPDL3280A in cancer patients. *Nature*. 2014;515:563–567. doi:10.1038/nature14011.
- Fehrenbacher L, Spira A, Ballinger M, Kowanzet M, Vansteenkiste J, Mazieres J, Park K, Smith D, Artal-Cortes A, Lewanski C, et al. Atezolizumab versus docetaxel for patients with previously treated non-small-cell lung cancer (POPLAR): a multicentre, open-label, phase 2 randomised controlled trial. *Lancet*. 2016;387:1837–1846. doi:10.1016/S0140-6736(16)00587-0.
- Jacquelot N, Roberti MP, Enot DP, Rusakiewicz S, Ternès N, Jegou S, Woods DM, Sodrè AL, Hansen M, Meirou Y, et al. Predictors of responses to immune checkpoint blockade in advanced melanoma. *Nat Commun*. 2017;8:592. doi:10.1038/s41467-017-00608-2.
- Fukuhara H, Ino Y, Todo T. Oncolytic virus therapy: A new era of cancer treatment at dawn. *Cancer Sci*. 2016;107:1373–1379. doi:10.1111/cas.13027.
- Hemminki O, Hemminki A. A century of oncolysis evolves into oncolytic immunotherapy. *Oncoimmunology*. 2016;5:e1074377. doi:10.1080/2162402X.2015.1074377.
- Bommareddy PK, Shettigar M, Kaufman HL. Integrating oncolytic viruses in combination cancer immunotherapy. *Nat Rev Immunol*. 2018;18:498–513. doi:10.1038/s41577-018-0014-6.
- Santos JM, Cervera-Carrascon V, Havunen R, Zafar S, Siurala M, Sorsa S, Anttila M, Kanerva A, Hemminki A. Adenovirus coding for interleukin-2 and tumor necrosis factor alpha replaces lymphodepleting chemotherapy in adoptive T cell therapy. *Mol Ther*. 2018;26:2243–2254. doi:10.1016/j.ymt.2018.06.001.
- Watanabe K, Luo Y, Da T, Guedan S, Ruella M, Scholler J, Keith B, Young RM, Engels B, Sorsa S, et al. Pancreatic cancer therapy with combined mesothelin-redirected chimeric antigen receptor T cells and cytokine-armed oncolytic adenoviruses. *JCI Insight*. 2018;3(7):e99573.
- Cervera-Carrascon V, Siurala M, Santos JM, Havunen R, Tahtinen S, Karell P, Sorsa S, Kanerva A, Hemminki A. TNFa and IL-2 armed adenoviruses enable complete responses by anti-PD-1 checkpoint blockade. *Oncoimmunology*. 2018;7:e1412902. doi:10.1080/2162402X.2017.1412902.
- Havunen R, Siurala M, Sorsa S, Gronberg-Vaha-Koskela S, Behr M, Tahtinen S, Santos JM, Karell P, Rusanen J, Nettelbeck DM, et al. Oncolytic adenoviruses armed with tumor necrosis factor alpha and interleukin-2 enable successful adoptive cell therapy. *Mol Ther Oncolytics*. 2017;4:77–86. doi:10.1016/j.omto.2016.12.004.
- Tahtinen S, Kaikkonen S, Merisalo-Soikkeli M, Gronberg-Vaha-Koskela S, Kanerva A, Parvainen S, Parvainen S, Vaha-Koskela M, Hemminki A. Favorable alteration of tumor microenvironment by immunomodulatory cytokines for efficient T-cell therapy in solid tumors. *PLoS One*. 2015;10:e0131242. doi:10.1371/journal.pone.0131242.
- Siurala M, Havunen R, Saha D, Lumen D, Airaksinen AJ, Tahtinen S, Cervera-Carrascon V, Bramante S, Parvainen S, Vaha-Koskela M, et al. Adenoviral delivery of tumor necrosis factor-alpha and interleukin-2 enables successful adoptive cell therapy of immunosuppressive melanoma. *Mol Ther*. 2016;24:1435–1443. doi:10.1038/mt.2016.137.
- Santos JM, Heinio C, Cervera-Carrascon V, Quixabeira DCA, Siurala M, Havunen R, Butzow R, Zafar S, de Grujil T, Lassus H, et al. Oncolytic adenovirus shapes the ovarian tumor microenvironment for potent tumor-infiltrating lymphocyte tumor reactivity. *J Immunother Cancer*. 2020;8:e000188.
- Santos JM, Havunen R, Siurala M, Cervera-Carrascon V, Tahtinen S, Sorsa S, Anttila M, Karell P, Kanerva A, Hemminki A. Adenoviral production of interleukin-2 at the tumor site removes the need for systemic postconditioning in adoptive cell therapy. *Int J Cancer*. 2017;141:1458–1468. doi:10.1002/ijc.30839.
- Kim TJ, Cho KS, Koo KC, Status C. Future perspectives of immunotherapy for locally advanced or metastatic urothelial carcinoma: a comprehensive review. *Cancers (Basel)*. 2020;12. doi:10.3390/cancers12010192.
- Rini BI, Powles T, Atkins MB, Escudier B, McDermott DF, Suarez C, Bracarda S, Stadler WM, Donskov F, Lee JL, et al. Atezolizumab plus bevacizumab versus sunitinib in patients with previously untreated metastatic renal cell carcinoma (IMmotion151): a multicentre, open-label, phase 3, randomised controlled trial. *Lancet*. 2019;393:2404–2415. doi:10.1016/S0140-6736(19)30723-8.
- Bronger H, Singer J, Windmuller C, Reuning U, Zech D, Delbridge C, Dorn J, Kiechle M, Schmalfeldt B, Schmitt M, et al. CXCL9 and CXCL10 predict survival and are regulated by cyclooxygenase inhibition in advanced serous ovarian cancer. *Br J Cancer*. 2016;115:553–563. doi:10.1038/bjc.2016.172.
- Hugo W, Zaretsky JM, Sun L, Song C, Moreno BH, Hu-Lieskova S, Berent-Maoz B, Pang J, Chmielowski B, Cherry G, et al. Genomic and transcriptomic features of response to anti-PD-1 therapy in metastatic melanoma. *Cell*. 2016;165:35–44. doi:10.1016/j.cell.2016.02.065.
- Rizvi NA, Hellmann MD, Snyder A, Kvistborg P, Makarov V, Havel JJ, Lee W, Yuan J, Wong P, Ho TS, et al. Cancer immunology. Mutational landscape determines sensitivity to PD-1 blockade in non-small cell lung cancer. *Science*. 2015;348:124–128. doi:10.1126/science.aaa1348.

31. Nesslinger NJ, Ng A, Tsang K-Y, Ferrara T, Schlom J, Gulley JL, Nelson BH. A viral vaccine encoding prostate-specific antigen induces antigen spreading to a common set of self-proteins in prostate cancer patients. *Clin Cancer Res.* 2010;16:4046–4056. doi:10.1158/1078-0432.CCR-10-0948.
32. Russell SJ, Peng K-W. Oncolytic virotherapy: a contest between apples and oranges. *Mole Ther.* 2017;25:1107–1116. doi:10.1016/j.ymthe.2017.03.026.
33. Silva MA, Ryall KA, Wilm C, Caldara J, Grote HJ, Patterson-Kane JC. PD-L1 immunostaining scoring for non-small cell lung cancer based on immunosurveillance parameters. *PLoS One.* 2018;13:e0196464. doi:10.1371/journal.pone.0196464.
34. Taube JM, Klein A, Brahmer JR, Xu H, Pan X, Kim JH, Chen L, Pardoll DM, Topalian SL, Anders RA. Association of PD-1, PD-1 ligands, and other features of the tumor immune microenvironment with response to anti-PD-1 therapy. *Clin Cancer Res.* 2014;20:5064–5074. doi:10.1158/1078-0432.CCR-13-3271.
35. Kowanetz M, Zou W, Gettinger SN, Koeppen H, Kockx M, Schmid P, Kadel EE 3rd, Wistuba I, Chaff J, Rizvi NA, et al. Differential regulation of PD-L1 expression by immune and tumor cells in NSCLC and the response to treatment with atezolizumab (anti-PD-L1). *Proc Natl Acad Sci U S A.* 2018. doi:10.1073/pnas.1802166115.
36. Zamarin D, Ricca JM, Sadekova S, Oseledchik A, Yu Y, Blumenschein WM, Wong J, Gigoux M, Merghoub T, Wolchok JD. PD-L1 in tumor microenvironment mediates resistance to oncolytic immunotherapy. *J Clin Invest.* 2018;128:1413–1428. doi:10.1172/JCI98047.
37. Dahan R, Segal E, Engelhardt J, Selby M, Korman AJ, Ravetch JV. FcγRs modulate the anti-tumor activity of antibodies targeting the PD-1/PD-L1 AXIS. *Cancer Cell.* 2015;28:285–295. doi:10.1016/j.ccell.2015.08.004.
38. Chen CY, Hutzen B, Wedekind MF, Cripe TP. Oncolytic virus and PD-1/PD-L1 blockade combination therapy. *Oncolytic Virother.* 2018;7:65–77. doi:10.2147/OV.S145532.
39. G. Pol J, Lévesque S, Workenhe ST, Gujar S, Le Boeuf F, R. Clements D, Fahrner J-E, Fend L, C Bell J, L. Mossman K, Fucikova J, Spisek R, et al. Trial watch: oncolytic viro-immunotherapy of hematologic and solid tumors. *Oncoimmunology.* 2018;7:e1503032.
40. Ribas A, Dummer R, Puzanov I, VanderWalde A, Andtbacka RHI, Michielin O, Olszanski AJ, Malvey J, Cebon J, Fernandez E, et al. Oncolytic virotherapy promotes intratumoral T cell infiltration and improves anti-PD-1 immunotherapy. *Cell.* 2017;170(1109–1119):e10. doi:10.1016/j.cell.2017.08.027.
41. Quetglas JJ, Labiano S, Aznar MA, Bolanos E, Azpilikueta A, Rodriguez I, Casales E, Sanchez-Paulete AR, Segura V, Smerdou C, et al. Virotherapy with a Semliki forest virus-based vector encoding IL12 synergizes with PD-1/PD-L1 blockade. *Cancer Immunol Res.* 2015;3:449–454. doi:10.1158/2326-6066.CIR-14-0216.
42. Blair GE, Dixon SC, Griffiths SA, Zajdel ME. Restricted replication of human adenovirus type 5 in mouse cell lines. *Virus Res.* 1989;14:339–346. doi:10.1016/0168-1702(89)90026-9.
43. Siurala M, Vaha-Koskela M, Havunen R, Tahtinen S, Bramante S, Parviainen S, Mathis JM, Kanerva A, Hemminki A. Syngeneic syrian hamster tumors feature tumor-infiltrating lymphocytes allowing adoptive cell therapy enhanced by oncolytic adenovirus in a replication permissive setting. *Oncoimmunology.* 2016;5:e1136046. doi:10.1080/2162402X.2015.1136046.